Structural and Multidisciplinary Optimization (2018) 58:1673–1693
https://doi.org/10.1007/s00158-018-1991-6

RESEARCH PAPER

An improved two-stage framework of evidence-based design optimization

Jinhao Zhang[1] · Mi Xiao[1] · Liang Gao[1] · Haobo Qiu[1] · Zan Yang[1]

Received: 22 December 2017 / Revised: 10 April 2018 / Accepted: 11 April 2018 / Published online: 24 April 2018

Abstract

In this paper, an improved two-stage framework is presented to handle the evidence-based design optimization (EBDO) problem under epistemic uncertainty. The improvements include two aspects: (1) in the first stage, the equal areas method is employed to transform evidence variables into random variables, which avoids the assumption that unknown evidence variables and parameters obey the normal distribution. Then, a reliability-based design optimization (RBDO) problem with random variables is defined and solved by the sequential optimization and reliability assessment (SORA) method; (2) in the second stage, an improved algorithm is presented, which can calculate the plausibility of constraint violation more efficiently by continuously recording the minimum and maximum values of limit-state functions. The computational accuracy and efficiency of the improved framework are tested by numerical and engineering examples.

Keywords Evidence-based design optimization · Reliability-based design optimization · Epistemic uncertainty · Evidence theory · Reliability analysis

Nomenclature

RBDO	Reliability-based design optimization
EBDO	Evidence-based design optimization
FD	Frame of discernment
BPA	Basic probability assignment
Bel	Belief
Pl	Plausibility
SORA	Sequential optimization and reliability assessment
HMV	Hybrid mean value
MPTP	Minimum performance target point
PDF	Probability density function
RBF	Radial basis functions
ND	Normal distribution

Responsible Editor: Jianbin Du

✉ Mi Xiao
xiaomi@hust.edu.cn

[1] State Key Laboratory of Digital Manufacturing Equipment and Technology, Huazhong University of Science and Technology, Wuhan 430074, Hubei, China

1 Introduction

Uncertainties widely exist in practical engineering systems, such as manufacturing tolerances, changing environmental and operating conditions, and incomplete information. Currently, reliability-based design optimization (RBDO) gains great attentions in the field of design optimization under uncertainty. Generally, the uncertainty can be classified into two types: aleatory and epistemic (Oberkampf et al. 2001; Kiureghian and Ditlevsen 2009; Zhang and Huang 2010). Aleatory uncertainty is objective and irreducible, while epistemic uncertainty is subjective and reducible. Probability theory is effective and usually employed to quantify the aleatory uncertainty when sufficient data are available. So far, many well-developed probability methods have been found in this research field (Du and Chen 2004; Shan and Wang 2008; Youn et al. 2008; Wang and Wang 2014; Meng et al. 2015a; Huang et al. 2016). For epistemic uncertainty, due to insufficient data, incomplete information and lack of knowledge about the design variables and parameters, it will be inappropriate that the epistemic uncertainty is simply treated as the aleatory one with assumed and inaccurate probability distributions (Yao et al. 2013). In this paper, the RBDO under epistemic uncertainty is focused on.

In RBDO, three important essentials need to be handled: uncertainty quantification, reliability analysis and optimization. Uncertainty quantification is the basis of reliability analysis and optimization. Many theories have been adopted to quantify epistemic uncertainty, such as evidence theory (Shafer 1976; Yang et al. 2016), fuzzy sets (Zadeh 1965; Huang and Zhang 2009; Li et al. 2015), convex models (Jiang et al. 2013a; Yang et al. 2015), and interval method (Moore 1966; Wu et al. 2013; Li et al. 2013). Among these theories, evidence theory seems to be more flexible and of wider applicability than the others in the quantification of epistemic uncertainty (Oberkampf and Helton 2002). It employs belief (*Bel*) and plausibility (*Pl*) to measure the likelihood of events. Specifically, the *Bel* and *Pl* are lower and upper bounds of the probability of an event. When they are equal, equivalent descriptions can be provided by evidence theory compared to the conventional probability theory. In fact, probability theory can be considered as a special case of evidence theory, and evidence theory can be equivalent to fuzzy sets, convex models, and possibility theory under some other special circumstances (Bae et al. 2004a).

Due to the above merits, evidence theory has been extensively used for epistemic uncertainty analysis. Oberkampf and Helton (2002) investigate the reliability analysis by using evidence theory for epistemic uncertainty. Bae et al. (2004a, 2004b) adopt evidence theory to handle epistemic uncertainty analysis for engineering structures. And a computational efficient method based on multi-point approximation (MPA) is proposed to alleviate the computational effort. Agarwal et al. (2004) utilize evidence theory to quantify epistemic uncertainty in multidisciplinary systems analysis. Du (2006, 2008) investigates the unified uncertainty analysis framework to handle both aleatory and epistemic uncertainties by probability and evidence theories. Additionally, if limit-state functions are implicit or computationally expensive, e.g., running computer-based simulations to obtain system state responses, metamodels can be constructed to replace the actual limit-state functions in reliability analysis using evidence theory. Bai et al. (2012) utilize quadratic polynomial without cross terms, radial basis functions (RBF) and high-dimensional model representation combined with moving least square to replace the implicit limit-state function in reliability analysis using evidence theory. Jiang et al. (2013b) adopt a uniformity approach to deal with the evidence variables, and then the most probable focal element is searched for constructing the approximate model of the limit-state function. Zhang et al. (2014) develop a sequential method to establish the response surface of the limit-state function based on control points in uncertainty domain of evidence variables, which have a significant contribution to the accuracy of response surface. Zhang et al. (2015) propose the first and second order approximate reliability analysis methods based on the most probable focal element using evidence theory. Xiao et al. (2015) propose an efficient method for reliability analysis under epistemic uncertainty based on evidence theory and support vector regression. Yang et al. (2017) perform the structural reliability analysis under evidence theory using the active learning kriging model.

Meanwhile, evidence theory is also used in the reliability optimization under epistemic uncertainty. The evidence-based design optimization (EBDO) has attracted attentions. Alyanak et al. (2008) propose an EBDO method based on the gradient information of the limit-state function. The method assumes that the gradient information can be determined by the finite difference method, and realizes the optimization by calculating the sensitivity of the limit-state function. Salehghaffari et al. (2013) utilize a response surface model to decrease the computational cost in the EBDO of a circular tube structure under axial impact load. Srivastava et al. (2013) propose a bi-objective evolutionary algorithm based approach to perform EBDO and make the first attempt to combine evidence theory with an evolutionary algorithm. Huang et al. (2013) conduct a review of general topics about the possibility and evidence-based reliability analysis and design optimization. Based on the first-order approximate reliability analysis method, Huang et al. (2017) propose a decoupling approach for EBDO.

Besides, Mourelatos and Zhou (2006) propose a computationally efficient two-stage method for EBDO under epistemic uncertainty. In the first stage of this method, RBDO is implemented to quickly identify the vicinity of the EBDO optimum with assuming that evidence variables and parameters obey the normal distribution. In the second stage, a derivative-free optimizer, i.e., the DIRECT, is used to calculate the EBDO optimum, starting from the obtained RBDO optimum in the first stage. If the basic probability assignments (BPA) of evidence variables and parameters are similar to the hypothetical normal distributions, a RBDO optimum in the vicinity of the final EBDO optimum can be easily obtained in the first stage of the method. Then, the EBDO optimum can be quickly found with few iterations in the second stage. However, if the BPAs are obviously different from normal distributions, under the assumption in the first stage, the obtained RBDO optimum may be far away from the final EBDO optimum. Then, the second stage still requires many iterations to search for the EBDO optimum. It is noteworthy that the *Pl* of constraint violation must be calculated every time when the optimizer evaluates a constraint in the second stage. The increased iterations in the second stage will incur more computational cost. In practical engineering problems, the BPAs are

complex and diverse, which are often different from the normal distributions. Therefore, the assumption in the first stage may make the two-stage EBDO method lose the expected computational efficiency.

To ensure a design point in the vicinity of the final EBDO optimum for all cases of BPAs, it is necessary to get rid of the assumption that unknown evidence variables and parameters obey the normal distribution. Thus, the first stage of the EBDO method proposed by Mourelatos and Zhou (2006) is modified in this work. The equal areas method (Xiao et al. 2015) is utilized to transform evidence variables into random variables. Then, a RBDO problem is defined and solved by the well-known sequential optimization and reliability assessment (SORA) method in the first stage.

On the other side, as mentioned above, the *Pl* of constraint violation must be calculated every time in the second stage of the method in Mourelatos and Zhou (2006). The efficiency of the corresponding algorithm used in their method is focused on in this work. An improved algorithm is presented, which can calculate the *Pl* of constraint violation more efficiently in the second stage by continuously recording the minimum and maximum values of limit-state functions.

Thus, based on the two-stage EBDO method in Mourelatos and Zhou (2006), the two above modifications are made in this paper. Namely, an improved two-stage framework of EBDO is presented. Numerical and engineering examples are provided to test the improved two-stage framework of EBDO. Results show that the improved framework can eliminate the limitation of the aforementioned hypothetical normal distribution and obtain a good EBDO optimum. Meanwhile, the improved framework is computationally more efficient, especially in terms of the reduction of evaluation times of limit-state functions during calculating the *Pl* of failure.

2 Common concepts in evidence theory and the EBDO model

In this section, evidence theory and reliability analysis using evidence theory are introduced in Sections 2.1 and 2.2, respectively. Section 2.3 describes the EBDO mathematical model.

2.1 Evidence theory

Evidence theory employs two measures to quantify the uncertainty of one proposition: *Bel* and *Pl*, which can be regarded as the lower and upper bounds of a probability measure and together structure the true probability instead of assigning a precise probability for a proposition (Yager et al. 1994). Some significant concepts of evidence theory are afforded as follows:

(1) Frame of discernment (*FD*): It is a set of mutually independent and disjoint elementary propositions. If a *FD* $X = \{x_1, x_2\}$, all the possible subsets of X will form a power set $\Omega(X) = 2^X = \{\Phi, \{x_1\}, \{x_2\}, \{x_1, x_2\}\}$, where Φ denotes the empty set. When X has n elements, $\Omega(X)$ will contain 2^n elements.

(2) Basic probability assignment (BPA): It is a mapping function $m : \Omega(X) \rightarrow [0, 1]$. Evidence theory assigns a belief mass to each element in the $\Omega(X)$ by BPA, which has to satisfy the following three conditions:

$$m(A) \geq 0 \qquad \text{for any } A \in \Omega(X) \tag{1}$$

$$m(\Phi) = 0 \tag{2}$$

$$\sum m(A) = 1 \qquad \text{for any } A \in \Omega(X) \tag{3}$$

where A is the focal element in evidence theory and $m(A)$ is the BPA for the focal element A.

(3) Belief (*Bel*) and plausibility (*Pl*): The *Bel* of an event refers to the sum of belief masses of all the propositions that totally support the event. It can be evaluated by the sum of BPAs of all the subsets of the event. The *Pl* of an event refers to the sum of belief masses of the propositions that agree with the event totally and partially. It is calculated by the sum of BPAs of all the sets which intersect with the event. For an event A, the $Bel(A)$ and $Pl(A)$ can be gained as

$$Bel(A) = \sum_{B \subseteq A} m(B) \tag{4}$$

$$Pl(A) = \sum_{B \cap A \neq \Phi} m(B) \tag{5}$$

(4) *Combination rules*: If there are multiple evidence sources to evaluate the $Bel(A)$ and $Pl(A)$, such as experts' opinions and experimental data, these sources should be combined by a certain rules. Dempster's rule is most popular rule for the combination (Sentz and Ferson 2002). For two events B and C with BPAs $m_1(B)$ and $m_2(C)$, the BPA of the combined evidence can be computed as

$$m(A) = \begin{cases} \dfrac{1}{1-k} \sum\limits_{B \cap C = A} m_1(B) m_2(C), & \text{for } A \neq \Phi \\ 0, & \text{for } A = \Phi \end{cases} \tag{6}$$

$$k = \sum_{B \cap C = \Phi} m_1(B) m_2(C) \tag{7}$$

where k refers to the conflict between two independent evidence sources. There are also other combination rules that can be found in (Yager et al. 1994; Sentz and Ferson 2002).

2.2 Reliability analysis using evidence theory

Consider the reliability analysis of the following limit-state function:

$$y = g(x_1, x_2), \qquad x_1 \in X_1, x_2 \in X_2 \tag{8}$$

where x_1 and x_2 are two independent uncertain variables and g is the limit-state function. Assume the failure region F is defined as

$$F = \{g : g(x_1, x_2) < 0\} \tag{9}$$

According to the evidence theory, the failure probability $p_f = P(g < 0)$ will be bracketed by $Bel(F)$ and $Pl(F)$.

$$Bel(F) \le p_f = P(\mathrm{g} < 0) \le Pl(F) \tag{10}$$

In this study, we assume that a combined BPA for each variable and parameter is provided, and each focal element is a closed interval. For two independent uncertain variables x_1 and x_2, a joint BPA in evidence theory can be gained by (11), which is similar to the joint probability in probability theory.

$$m(C) = m(A) \times m(B) \qquad \text{when } C \in A \times B \tag{11}$$

where $A \in \Omega(X_1)$ and $B \in \Omega(X_2)$, and C is a focal element of the Cartesian product $A \times B$, which is defined by:

$$A \times B = \{x = [x_1, x_2], x_1 \in A, x_2 \in B\} \tag{12}$$

Based on the joint BPA $m(C)$, $Bel(F)$ and $Pl(F)$ can be calculated by determining whether $C \subseteq F$ or $C \cap F \neq \Phi$. For the failure region F, if the focal element C is wholly in the domain $g(x_1, x_2) < 0$, $C \subseteq F$; if the focal element C is entirely or partially within the domain $g(x_1, x_2) < 0$, $C \cap F \neq \Phi$. These judgments can be made by calculating the extreme value of the limit-state function g over each focal element, namely

$$[g_{\min}, g_{\max}] = \left[\min_{X \in C_k} g(X), \max_{X \in C_k} g(X)\right], \qquad k = 1, \ldots, n \tag{13}$$

where C_k represents a focal element and n is the total number of focal elements. g_{min} and g_{max} can be gained by the vertex method or the gradient-based optimization method. Figure 1 schematically shows three types of focal elements for the calculation of $Bel(F)$ and $Pl(F)$ (Mourelatos and Zhou 2006). For type 1, g_{min} is negative and g_{max} are positive, the focal element will only contribute to $Pl(F)$. For type 2, both g_{min} and g_{max} are positive, the focal element will not contribute to $Bel(F)$ or $Pl(F)$. For type 3, both g_{min} and g_{max} are negative, the focal element will contribute to $Bel(F)$ and $Pl(F)$.

2.3 EBDO model

The mathematical model of the EBDO problem can be typically formulated as follows:

$$\begin{aligned} &find: \quad \boldsymbol{d}, \boldsymbol{e_X} \\ &\min: \quad f(\boldsymbol{d}, \boldsymbol{e_X}, \boldsymbol{e_P}) \\ &s.t. \quad Pl(g_i(\boldsymbol{d}, \boldsymbol{X}, \boldsymbol{P}) < 0) \le p_{f_i}, \qquad i = 1, 2, \cdots, N \\ &\qquad \boldsymbol{d}^L \le \boldsymbol{d} \le \boldsymbol{d}^U, \boldsymbol{e}_{\boldsymbol{X}}^L \le \boldsymbol{e_X} \le \boldsymbol{e}_{\boldsymbol{X}}^U \end{aligned} \tag{14}$$

where f is the objective function, g_i is the ith constraint, and N is the number of constraints. $\boldsymbol{d}$ is the vector of deterministic variables, $\boldsymbol{X}$ is the vector of evidence variables, $\boldsymbol{P}$ is the vector of evidence parameters, $\boldsymbol{e_X}$ and $\boldsymbol{e_P}$ are the nominal value vectors of evidence variables and parameters, respectively. Pl denotes the plausibility of constraint violation. p_{f_i} is an acceptable value of the plausibility of the ith constraint violation. $\boldsymbol{d}^L$, $\boldsymbol{d}^U$, $\boldsymbol{e}_{\boldsymbol{X}}^L$, and $\boldsymbol{e}_{\boldsymbol{X}}^U$ are the lower and upper bounds of deterministic variables and evidence variables, respectively.

3 The improved two-stage framework of EBDO

To solve the EBDO problem with epistemic uncertainty in (14), Mourelatos and Zhou (2006) propose a two-stage method. In this method, an initial design point is moved to the vicinity of the EBDO optimum in the first stage before calculating the Pl of constraint violation in the second stage. To alleviate the computational effort in the first stage, the movement of a hyperellipse which contains the FD is employed and realized by solving a RBDO problem. The center of the hyperellipse is an approximate design point. In their method, it needs to be assumed that each dimension of the FD is equal to some times the standard derivation of a hypothetical normal distribution, such as six times. To avoid this assumption, the equal areas method (Xiao et al. 2015) is introduced to transform evidence variables into random variables. Then, a RBDO problem is defined and solved by SORA in the first stage. On the other hand, an improved algorithm for more efficiently calculating the Pl of constraint violation in the second stage is presented to decrease the evaluation times of the limit-state function, therefore saving the computational cost. The improved two-stage framework of EBDO will be elaborated in the following sections.

3.1 The first stage of the improved EBDO framework

In the first stage of the improved two-stage framework, the equal areas method is used to transform evidence variables

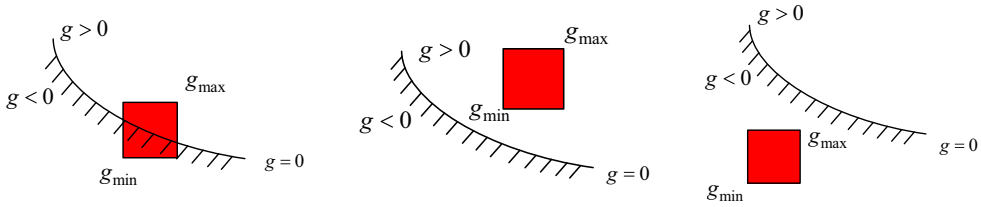

Fig. 1 Contribution of a focal element to *Bel* and *Pl*

into random variables. Using this method, the assumption is avoided that each dimension of the *FD* is equal to some times the standard derivation of a hypothetical normal distribution. In the remainder of this section, we will briefly introduce the key points involved in the first stage of the improved framework.

3.1.1 Reliability analysis based on hybrid mean value

At the beginning, evidence variables are transformed into random variables by the method based on equal areas (Xiao et al. 2015). As illustrated in Fig. 2, the probability density $f(y = L_1)$ is set as follows:

$$f(y = L_1) = \frac{m(A_1)}{2(U_1 - L_1)} \tag{15}$$

where y denotes the non-normal random variable from the transformation of the evidence variable x, L_1 and U_1 are the lower and upper bounds of the interval A_1. In Fig. 2, the area $S_{A_{11}}$ of the domain A_{11} is equal to the area $S_{A_{12}}$ of the domain A_{12}. Then, the probability density $f(y = U_1)$ can be computed. Equation (16) can be used to calculate the probability densities $f(y = U_i, i = 1, 2, \ldots, 6)$. Thus, the random variable and its probability density function (PDF) can be obtained.

$$f(y = U_i) = \frac{2m(A_i)}{U_i - L_i} - f(y = L_i), \qquad i = 1, 2, \ldots, 6 \tag{16}$$

For ease of calculation of the probability density and cumulative probability density of a random variable during reliability analysis, the metamodel is created to replace the piecewise linear PDF of the random variable. Each interval bound of the evidence variable and its corresponding probability density can be viewed as the sample data, i.e., the sample points $B_i (i = 1, 2, \ldots, 7)$ in Fig. 2. Based on the sample data, the metamodel can be constructed. In this study, the RBF metamodeling technique is employed. RBF is originally developed to implement the interpolation of scattered multivariate data by using the linear combination of radially symmetric functions (Hardy 1971). The RBF metamodel used in this paper is described as

$$y = w_0 + \sum_{i=1}^{n} w_i \varphi(\|x - x_i\|) \tag{17}$$

where w_0 is a polynomial function and w_i denotes the coefficient determined by least squares estimation. x_i is a central point obtained from the sample data and φ is a basis function which has multiple forms such as linear function, multiquadric, inverse multiquadric, thin plate spline and Gaussian. In this study, the linear basis function is employed and it takes the following form:

$$\varphi = \|x - x_i\| \tag{18}$$

After the aforementioned transformation, the reliability analysis can be conducted. Many methods have been developed for the reliability analysis with random variables, such as the hybrid mean value (HMV; Youn et al. 2003), modified chaos control (Meng et al. 2015b), step length adjustment

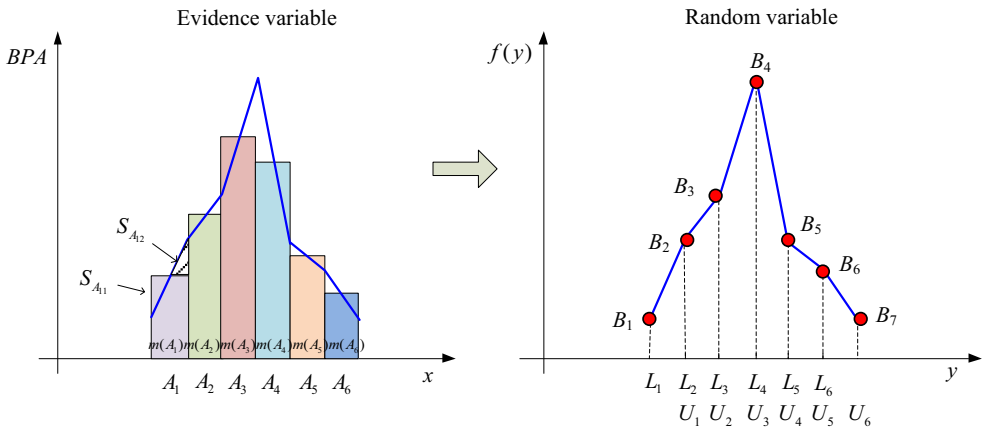

Fig. 2 Transformation of an evidence variable into a random variable

Fig. 3 The pseudocode of the improved algorithm

Step 1: Set $PF=\{FD\}$ and $TF=\{0\}$ and counter m=1.
Step 2: Calculate the $g^r_{\min}$ and $g^r_{\max}$ of PF, and record their locations $\boldsymbol{X}^r_{\min}$ and $\boldsymbol{X}^r_{\max}$.
Step 3: Consider all sets $D_k : D_k \subset PF$ *or* $D_k \subseteq PF$.
Set counter n=0.
Set PF={0}.
For k=1 to m
Partition D_k into D^1_k and D^2_k.
For t=1 to 2
If $\boldsymbol{X}^r_{\min}$ is in the D^t_k **then**
$g_{\min}(D^t_k) = g^r_{\min}$.
Else
Calculate $g_{\min}(D^t_k)$ and update $g^r_{\min}$, i.e., $g^r_{\min} = g_{\min}(D^t_k)$.
End If (the loop of $\boldsymbol{X}^r_{\min}$ in the D^t_k)
If $g_{\min}(D^t_k) < 0$ **then**
If $\boldsymbol{X}^r_{\max}$ is in the D^t_k **then**
$g_{\max}(D^t_k) = g^r_{\max}$.
Else
Calculate $g_{\max}(D^t_k)$ and update $g^r_{\max}$, i.e., $g^r_{\max} = g_{\max}(D^t_k)$.
End If (the loop $\boldsymbol{X}^r_{\max}$ in the D^t_k)
If $g_{\max}(D^t_k) > 0$ **then**
$PF = PF \bigcup D^t_k$ and $n = n$+1.
Else
$TF = TF \bigcup D^t_k$.
End If (the loop of $g_{\max}(D^t_k) > 0$)
End If (the loop of $g_{\min}(D^t_k) < 0$)
End For (the loop of t=1 to 2)
End For (the loop of k= 1 to m)
Set counter m=n.
If PF can be partitioned, go to Step 3.
If PF cannot be partitioned, stop and calculate the PI of failure.

Fig. 4 Illustration of the improved algorithm for calculating the PI of failure

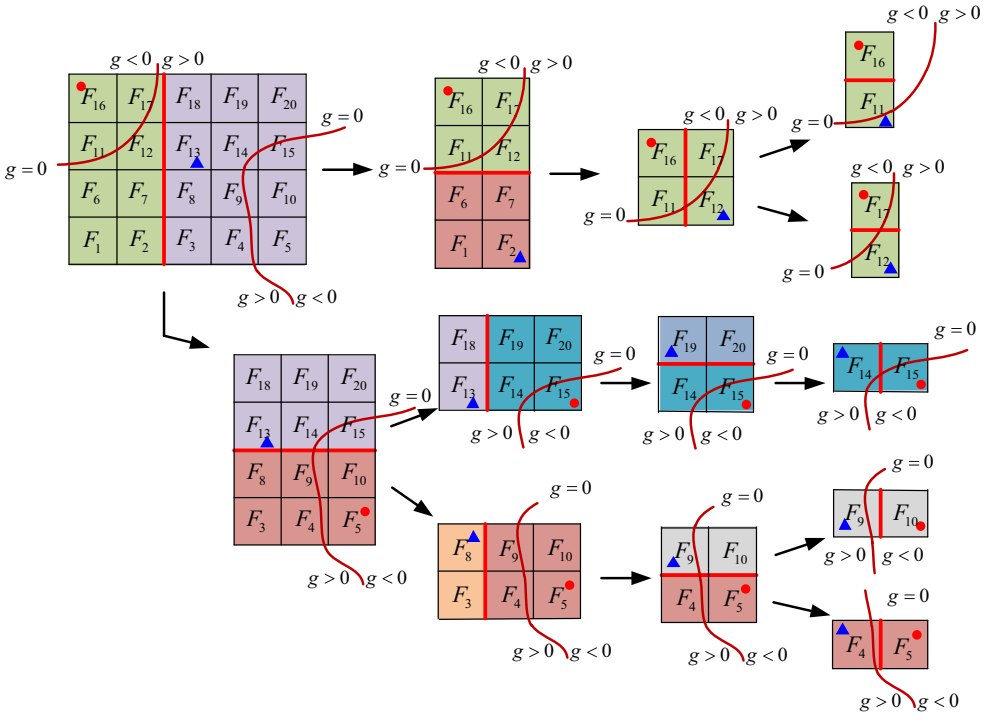

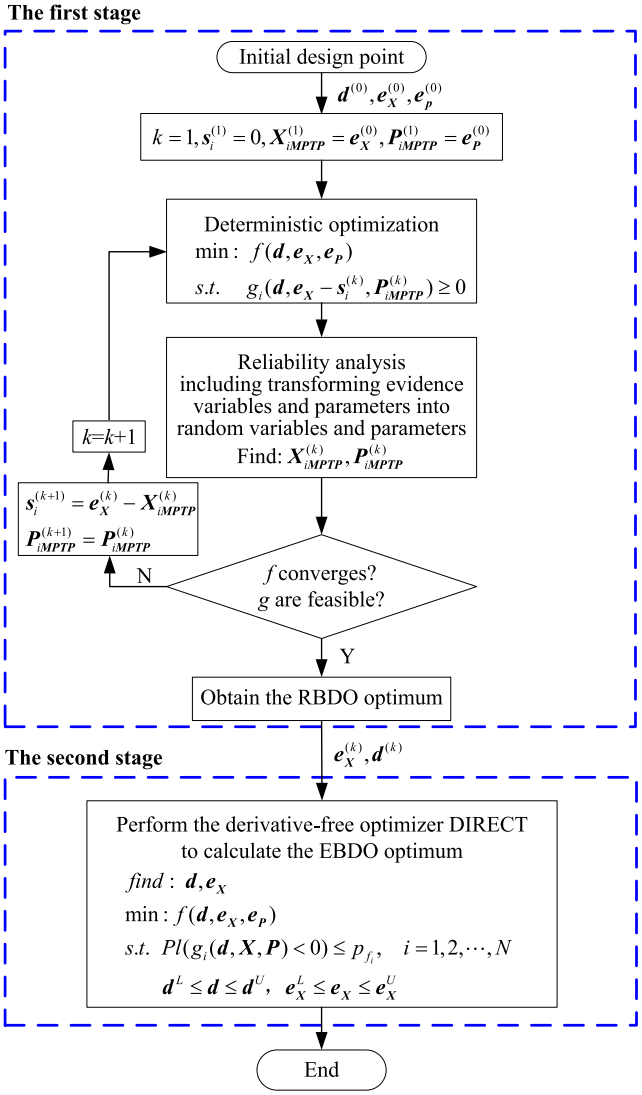

Fig. 5 Flowchart of the improved two-stage framework of EBDO

(Yi and Zhu 2016), and enhanced chaos control (ECC; Hao et al. 2017) methods. In this research, the traditional HMV method is used. Using this method, the minimum performance target point of the reliability analysis with random variables can be obtained by solving the optimization problem as below:

$$\begin{aligned} &\min: \quad G(\boldsymbol{U}) \\ &s.t. \quad \|\boldsymbol{U}\| = \beta^t \end{aligned} \tag{19}$$

where $G(\boldsymbol{U})$ denotes the limit-state function, $\boldsymbol{U}$ is the vector of the standard normal random variables, and β^t is the reliability index vector of $G(\boldsymbol{U})$ at the MPTP. In this paper, the non-normal random variables are converted into the standard normal random variables by the Rosenblatt transformation method (Rosenblatt 1952).

3.1.2 Searching for the RBDO optimum based on SORA

After the reliability analysis with transformed random variables, in this paper, the SORA method (Du and Chen 2004) is employed to solve the RBDO problem. In SORA, the solving process of RBDO is a sequential work of deterministic optimization and reliability analysis. As seen in (20), the probabilistic optimization is transformed into a deterministic optimization by shifting the limit-state function to the feasible region based on the offset vector and the minimum performance target point (MPTP) obtained by the reliability analysis in Section 3.1.1.

$$\begin{aligned} &find: \boldsymbol{d}, \boldsymbol{e_X} \\ &\min: \quad f(\boldsymbol{d}, \boldsymbol{e_X}, \boldsymbol{e_P}) \\ &s.t. \quad g_i\left(\boldsymbol{d}, \boldsymbol{e_X} - \boldsymbol{s_i}^{(k+1)}, \boldsymbol{P_{iMPTP}}^{(k)}\right) \geq 0, \quad i = 1, 2, \cdots, N \\ &\quad \boldsymbol{s_i}^{(k+1)} = \boldsymbol{e_X}^{(k)} - \boldsymbol{X_{iMPTP}}^{(k)} \\ &\quad \boldsymbol{d}^L \leq \boldsymbol{d} \leq \boldsymbol{d}^U, \quad \boldsymbol{e_X^L} \leq \boldsymbol{e_X} \leq \boldsymbol{e_X^U} \end{aligned} \tag{20}$$

where $\boldsymbol{d}$ is the vector of deterministic variables, $\boldsymbol{X}$ and $\boldsymbol{P}$ are the vectors of random variables and parameters after the transformation. $\boldsymbol{e_X}$ and $\boldsymbol{e_P}$ are the nominal value vectors of random variables and parameters, respectively. $\boldsymbol{s}_i^{(k+1)}$ is the offset vector of the ith constraint at the $(k+1)$th iteration of SORA. $\boldsymbol{e}_X^{(k)}$ is the optimum of the deterministic optimization at the kth iteration. $\boldsymbol{X}_{iMPTP}^{(k)}$ and $\boldsymbol{P}_{iMPTP}^{(k)}$ are the MPTPs of the reliability analysis with random variables and parameters for the ith constraint at the kth iteration of SORA, respectively.

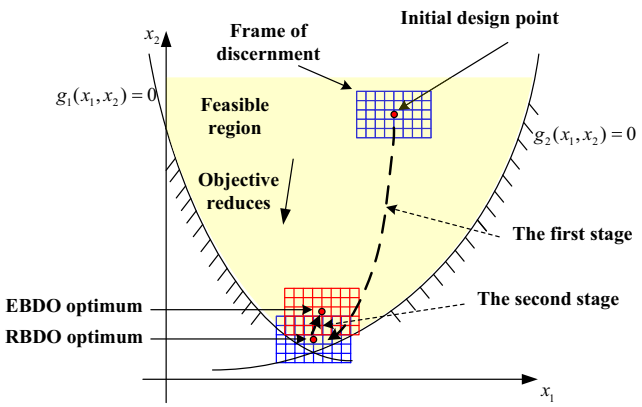

Fig. 6 Movements of *FD* under the improved two-stage framework of EBDO

3.2 An improved algorithm for calculating the *Pl* of failure in the second stage

In the second stage of the improved two-stage framework, the *Pl* of failure needs to be calculated every time the optimizer evaluates a constraint. Therefore, the efficiency of calculating the *Pl* of failure has a crucial

Table 1 BPA structures for x_1 and x_2

x_1		x_2	
Interval	BPA (%)	Interval	BPA (%)
$[e_{x_1} -0.9, e_{x_1} -0.6]$	10	$[e_{x_2} -0.9, e_{x_2} -0.6]$	5
$[e_{x_1} -0.6, e_{x_1} -0.3]$	20	$[e_{x_2} -0.6, e_{x_2} -0.3]$	20
$[e_{x_1} -0.3, e_{x_1}]$	25	$[e_{x_2} -0.3, e_{x_2}]$	25
$[e_{x_1}, e_{x_1} +0.3]$	20	$[e_{x_2}, e_{x_2} +0.3]$	20
$[e_{x_1} +0.3, e_{x_1} +0.6]$	15	$[e_{x_2} +0.3, e_{x_2} +0.6]$	15
$[e_{x_1} +0.6, e_{x_1} +0.9]$	10	$[e_{x_2} +0.6, e_{x_2} +0.9]$	15

effect on the efficiency of EBDO. Based on the algorithm in Mourelatos and Zhou (2006) for calculating the Pl of failure, an improved algorithm that records the minimum and maximum values of limit-state functions during optimization iterations is presented in this paper. Using this improved algorithm, the evaluation times of limit-state functions or constraints are reduced and the computational cost is saved. The pseudocode of the improved algorithm is shown in Fig. 3.

As shown in Fig. 3, a set PF is initially equal to the entire frame of discernment (FD). The minimum and maximum values of the limit-state function $g(\boldsymbol{X})$ in the set PF are evaluated and recorded as $g^r_{\min}$ and $g^r_{\max}$. Their corresponding locations in the set PF are recorded as $\boldsymbol{X}^r_{\min}$ and $\boldsymbol{X}^r_{\max}$. At the first iteration, the PF is partitioned into sets D^t ($t=1$ and 2). If $\boldsymbol{X}^r_{\min}$ locates in the set D^t, the recorded value $g^r_{\min}$ will be assigned to the minimum value of $g(\boldsymbol{X})$ in this set, i.e., $g_{\min}(D^t) = g^r_{\min}$. Similarly, if $\boldsymbol{X}^r_{\max}$ locates in the region D^t, $g_{\max}(D^t) = g^r_{\max}$. If $\boldsymbol{X}^r_{\min}$ or $\boldsymbol{X}^r_{\max}$ locates outside the set D^t, $g_{\min}(D^t)$ or $g_{\max}(D^t)$ will be calculated. Then, $g^r_{\min}$, $g^r_{\max}$ and their corresponding locations $\boldsymbol{X}^r_{\min}$ and $\boldsymbol{X}^r_{\max}$ in the set D^t are updated and recorded. If $g_{\min}(D^t) < 0$ and $g_{\max}(D^t) > 0$, D^t will be placed in the set PF. If $g_{\min}(D^t_k) < 0$ and $g_{\max}(D^t_k) \le 0$, D^t will be placed in the set TF. Otherwise, D^t will be eliminated and not considered further. Then, the second iteration begins. The above iteration process will not be stopped until the set PF cannot be partitioned. Finally, the Pl of failure can be computed by (21).

$$Pl(g < 0) = \sum_{E_1 \in PF} m(E_1) + \sum_{E_2 \in TF} m(E_2) \tag{21}$$

where the sets PF and TF are used to storage the focal elements with types 1 and 3 in Fig. 1, respectively. E_1 and E_2 denote the focal elements in the sets PF and TF, respectively.

In the above algorithm, if $g_{\min}(D^t)$ or $g_{\max}(D^t)$ cannot be directly assigned the recorded values, they can be calculated by the vertex method or the gradient-based

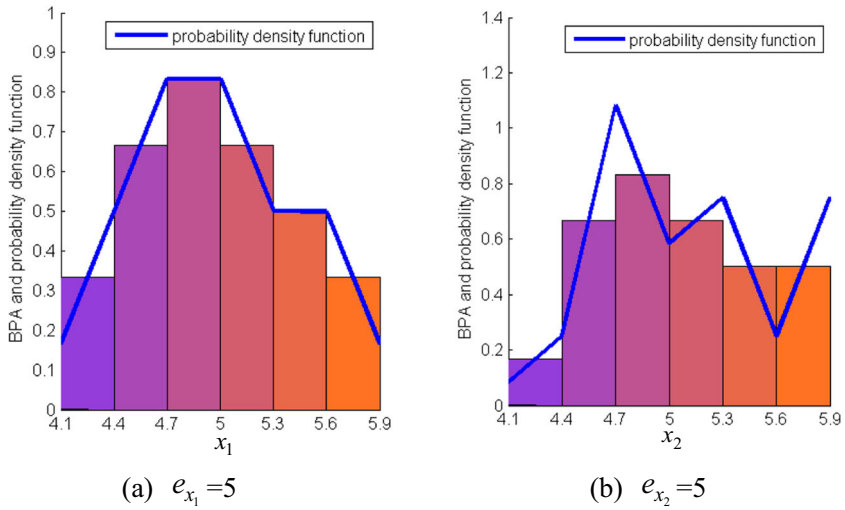

(a) e_{x_1}=5 (b) e_{x_2}=5

Fig. 7 BPA structures and the corresponding PDFs after transformation

Table 2 Comparative results under different cases in example 1

p_f	EBDO methods	Max iterations	RBDO optimum		EBDO optimum		EBDO objective	*Pl* of failure			Total number of function calls in each stage
			x_1	x_2	x_1	x_2	f	Pl_1	Pl_2	Pl_3	
0.01	One-stage	5	/	/	5	2.778	−1.410	0	0	0	1315
		50	/	/	4.490	2.222	−1.614	0.005	0.005	0	32,547
	Two-stage with ND	5	4.626	1.699	4.626	2.254	−1.600	0.005	0.005	0	1788 + 2313
	Improved two-stage	5	4.596	2.179	4.596	2.154	**−1.642**	0.005	0.005	0	4279 + 1359
0.1	One-stage	5	/	/	5	2.407	−1.545	0	0.0125	0	1415
		50	/	/	4.490	1.852	−1.777	0.0975	0.025	0	42,543
	Two-stage with ND	5	5.152	0.794	4.707	1.827	−1.783	0.0475	0.087	0	1274 + 3599
	Improved two-stage	5	4.553	1.849	4.620	1.760	**−1.815**	0.0975	0.0875	0	2494 + 1463
0.2	One-stage	5	/	/	5	2.407	−1.545	0	0.0125	0	1415
		50	/	/	4.763	1.482	−1.940	0.185	0.175	0	56,677
	Two-stage with ND	5	4.925	1.091	4.703	1.6827	−1.848	0.105	0.125	0	1522 + 3791
	Improved two-stage	5	4.667	1.455	4.867	1.450	**−1.952**	0.185	0.175	0	1431 + 2311

optimization method. Compared with the gradient-based optimization method, the vertex method is more efficient because it does not require the optimization solving process to search for the minimum and maximum values of a limit-state function. In the whole design space, the limit-state function may be nonlinear and non-monotonic. But in practical engineering problems, the range of *FD* is usually small. The nonlinearity of the limit-state function is not high in this small range and the limit-state function can be considered as monotonic. Then the vertex method can be employed. Additionally, for a *FD* composed of n evidence variables and parameters, an n-dimensional hyperrectangle can be used to represent this *FD*. The following partition scheme for the n-dimensional hyperrectangle is employed in the above improved algorithm. At the jth iteration ($j = 1,\ldots,n$), the hyperrectangle is partitioned into two parts by an (n-1)-dimensional hyperplane perpendicular to the jth dimension. Assuming that the evidence variable or parameter in the jth dimension has p focal elements, if p is an even number, the (n-1)-dimensional hyperplane will be located in between the (p/2)th and (p/2 + 1)th focal elements; if p is an odd number, the (n-1)-dimensional hyperplane will be located in between the (p/2–0.5)th and (p/2 + 0.5) focal elements. For the case that the hyperrectangle cannot be partitioned by the hyperplane perpendicular to the jth dimension, if $j < n$, the (j + 1)th dimension will be chosen; if $j = n$, the 1st dimension will be selected. After the nth dimension is chosen, the new dimension cycle in sequence will begin. The partition process will be terminated when the types of all focal elements are identified.

A limit state function with two disjoint failure domains is used to explain the developed algorithm. The *FD* and the limit-state function $g = 0$ are shown in Fig. 4. Each rectangle block in the *FD* denotes a focal element. The *FD* contains the total of 20 focal elements denoted by F_i, $i = 1, 2, \ldots, 20$. The red dots and blue triangles in Fig. 4 denote the minimum and maximum values (i.e., $g^r_{\min}$ and $g^r_{\max}$) in each set, respectively. At the first iteration, $g^r_{\min}$ and $g^r_{\max}$ in the *FD* are calculated and recorded. Simultaneously, their locations $\boldsymbol{X}^r_{\min}$ and $\boldsymbol{X}^r_{\max}$ are recorded. Then, the *FD* is partitioned into two sets by the red vertical line, including $D_1^1 = \cup F_i$, $i = 1, 2, 6, 7, 11, 12, 16, 17$, and $D_1^2 = \cup F_i$, $i = 3, 4, 5, 8, 9, 10, 13, 14, 15, 18, 19, 20$. It can be observed that $\boldsymbol{X}^r_{\min}$ and $\boldsymbol{X}^r_{\max}$ locates in D_1^1 and D_1^2, respectively. Thus, for D_1^1, it can be determined that $g_{\min}(D_1^1) = g^r_{\min}$; while $g_{\max}(D_1^1)$ needs to be calculated, i.e., $g_{\max}(D_1^1) = \max g(\boldsymbol{X}), \boldsymbol{X} \in D_1^1$. Similarly, for D_1^2, it can be judged that $g_{\max}(D_1^2) = g^r_{\max}$; while $g_{\min}(D_1^2)$ needs to be calculated, i.e.,

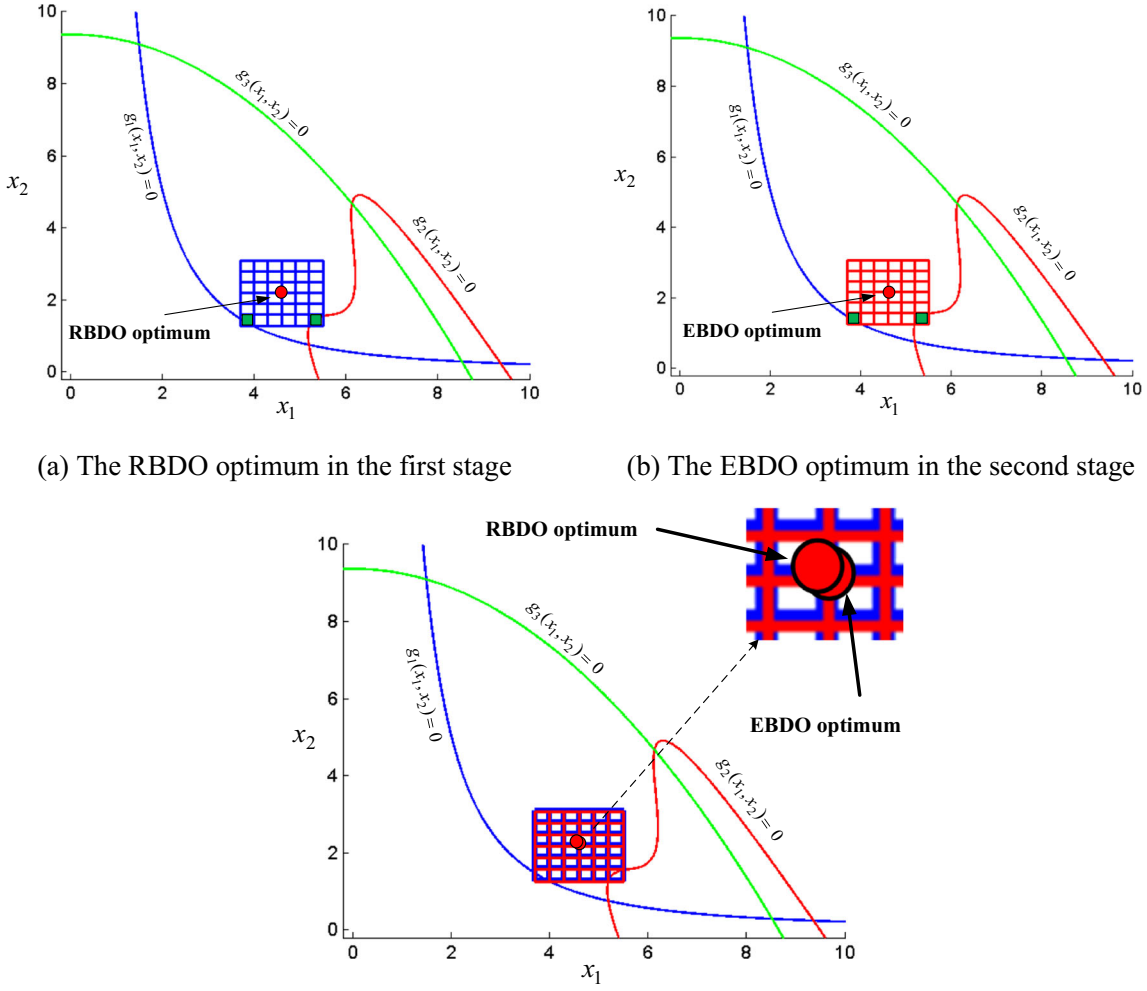

(a) The RBDO optimum in the first stage

(b) The EBDO optimum in the second stage

(c) Comparison of the RBDO and EBDO optimums

Fig. 8 Movements of *FD* under the improved two-stage framework of EBDO and $p_f = 0.01$ in example 1

$g_{\min}\left(D_1^2\right) = \min g(\boldsymbol{X}), \boldsymbol{X} \in D_1^2$. Because $g_{\min}\left(D_1^1\right) < 0$ and $g_{\max}\left(D_1^1\right) > 0$, D_1^1 is placed in the *PF*. Similarly, $g_{\min}\left(D_1^2\right) < 0$ and $g_{\max}\left(D_1^2\right) > 0$, D_1^2 is also placed in the *PF*. Then, the first iteration is finished.

Table 3 Comparison of efficiency for calculating *Pl* of failure in example 1

p_f	The vertex method				The gradient-based method			
	Algorithms of calculating *Pl* of failure	Number of each constraint function calls			Algorithms of calculating *Pl* of failure	Number of optimizer calls for each constraint		
		g_1	g_2	g_3		g_1	g_2	g_3
0.01	Algorithm involving all focal elements	144	144	144	Algorithm without records	12	15	2
	The improved algorithm	**12**	**14**	**6**	The improved algorithm	**9**	**11**	**2**
0.1	Algorithm involving all focal elements	144	144	144	Algorithm without records	41	28	2
	The improved algorithm	**28**	**20**	**6**	The improved algorithm	**26**	**17**	**2**
0.2	Algorithm involving all focal elements	144	144	144	Algorithm without records	54	36	2
	The improved algorithm	**34**	**24**	**6**	The improved algorithm	**32**	**21**	**2**

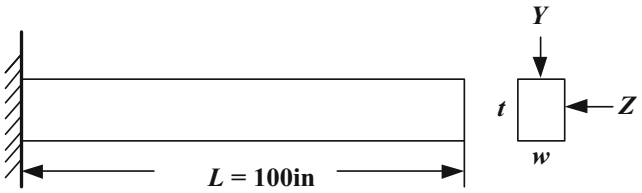

Fig. 9 Cantilever beam example

At the second iteration, D_1^1 is partitioned into $D_1^{11} = \cup F_i, i = 11, 12, 16, 17$ and $D_1^{12} = \cup F_i, i = 1, 2, 6, 7$. D_1^2 is partitioned into $D_1^{21} = \cup F_i, i = 13, 14, 15, 18, 19, 20$ and $D_1^{22} = \cup F_i, i = 3, 4, 5, 8, 9, 10$. After the judgment, D_1^{11}, D_1^{21} and D_1^{22} are placed in *PF* and D_1^{12} is discarded. At the third iteration, D_1^{11} is partitioned into $D_1^{111} = \cup F_i, i = 11, 16$ and $D_1^{112} = \cup F_i, i = 12, 17$. D_1^{21} is partitioned into $D_1^{211} = \cup F_i, i = 13, 18$, $D_1^{212} = \cup F_i, i = 14, 15, 19, 20$. D_1^{22} is partitioned into $D_1^{221} = \cup F_i, i = 3, 8$, $D_1^{222} = \cup F_i, i = 4, 5, 9, 10$. After the judgment, D_1^{111}, D_1^{112}, D_1^{212} and D_1^{222} are placed in *PF*, and D_1^{211} and D_1^{221} are discarded. After five iterations, the partition of the whole *FD* is finished. Finally, $TF = \{F_5, F_{10}, F_{16}\}$ and $PF = \{F_4, F_9, F_{11}, F_{12}, F_{14}, F_{15}, F_{17}\}$. The sum of BPA of all focal elements in *PF* and *TF* can be calculated and considered as the *Pl* of failure.

3.3 Flowchart of the improved two-stage framework

Figure 5 shows the flowchart of the improved two-stage framework of EBDO. The explanations of variables and parameters in this figure have been given after (14) and (20). In the first stage, evidence variables are transformed into random variables during the reliability analysis. Then the reliability analysis with random variables is conducted by the HMV method. The RBDO problem with random variables is solved by SORA. The gained RBDO optimum is viewed as the vicinity of the EBDO optimum. In the second stage, the EBDO problem is solved, in which the *Pl* of constraint violation is calculated and the RBDO optimum is considered as the initial design point. Generally, a derivative-free optimizer is required to solve the EBDO problem due to the discontinuous nature of the combined BPA structure (Mourelatos and Zhou 2006). In this research, the derivative-free global optimizer, i.e., the DIvisions of RECTangles (DIRECT), is used. DIRECT is a modification of the standard Lipschitzian approach that eliminates the need to specify a Lipschitz constant (Jones et al. 1993; Mourelatos and Zhou 2006). Evolutionary algorithms can be also utilized as the global optimizer, but large initial sample points are required.

The improved two-stage framework of EBDO is illustrated by a two-dimensional example in Fig. 6. The grid represents the *FD*, in which each block denotes one focal element. The red dot in the grid is an evidence design point.

4 Test examples

In this section, three numerical examples and an engineering example are presented to test the improved two-stage framework of EBDO.

4.1 A mathematical example

This example is modified from (Youn et al. 2005). The mathematical model of the EBDO problem is shown in (22). e_{x_1} and e_{x_2} denote the nominal values of evidence variables x_1 and x_2, respectively. To test the advantage of the improved method without the assumption that unknown evidence variables and parameters obey the normal distribution, the BPA structures for x_1 and x_2

Table 4 BPA structures for *Z*, *y*, *Y* and *E*

Z		*y* (×10^3)		*Y*		*E* (×10^6)	
Interval	BPA (%)	Interval	BPA (%)	Interval	BPA (%)	Interval	BPA (%)
[200, 300]	5	[35, 37]	5	[700, 800]	10	[26.5, 27.5]	10
[300, 400]	5	[37, 38]	5	[800, 900]	10	[27.5, 28.5]	10
[400, 450]	10	[38, 39]	10	[900, 1000]	30	[28.5, 29]	30
[450, 500]	30	[39, 40]	30	[1000, 1100]	30	[29, 29.5]	30
[500, 550]	30	[40, 41]	30	[1100, 1200]	10	[29.5, 30.5]	10
[550, 600]	10	[41, 42]	10	[1200, 1300]	10	[30.5, 31.5]	10
[600, 700]	5	[42, 43]	5				
[700, 800]	5	[43, 45]	5				

Table 5 Comparative results under different cases in example 2

p_f	EBDO methods	Max iterations	RBDO optimum		EBDO optimum		EBDO objective	*Pl* of failure		Total number of function calls in each stage
			w	t	w	t	f	Pl_1	Pl_2	
0.01	One-stage	10	/	/	2.473	3.920	9.692	0.009	0	21,863
		30	/	/	2.596	3.732	9.688	0.009	0	99,503
	Two-stage with ND	10	2.350	3.820	2.573	3.771	9.705	0.009	0	2032 + 42,095
	Improved two-stage	10	2.460	4.013	2.526	3.835	**9.687**	0.009	0	3098 + 15,613
0.1	One-stage	10	/	/	2.130	4.163	8.865	0.00985	0.0970	33,617
		30	/	/	2.154	4.112	8.856	0.09975	0.0635	171,443
	Two-stage with ND	10	2.057	3.764	2.426	3.657	8.873	0.0988	0.0215	2048 + 89,975
	Improved two-stage	10	2.346	3.871	2.265	3.908	**8.853**	0.09925	0.059	4093 + 58,431
0.2	One-stage	10	/	/	2.436	3.5265	8.591	0.1963	0.0465	47,013
		30	/	/	2.068	4.137	8.555	0.17225	0.16	239,701
	Two-stage with ND	10	2.109	3.854	2.059	4.154	8.581	0.1918	0.1910	1876 + 125,223
	Improved two-stage	10	2.117	3.933	2.125	4.014	**8.529**	0.19925	0.133	1319 + 100,623

are set to distinguish them from those with normal distribution (seen in Table 1).

$$
\begin{aligned}
&find: \quad e_{x_1}, e_{x_2}\\
&\min: \quad f(e_{x_1}, e_{x_2}) = -\frac{(e_{x_1}+e_{x_2}-10)^2}{30} - \frac{(e_{x_1}-e_{x_2}+10)^2}{120}\\
&s.t. \quad Pl\{g_i(x_1,\ x_2) < 0\} \le p_f, \qquad i = 1,2,3\\
&\qquad g_1 = \frac{x_1^2 x_2}{20} - 1\\
&\qquad g_2 = 1-(Y-6)^2 + (Y-6)^3 - 0.6(Y-6)^4 + Z\\
&\qquad g_3 = \frac{80}{x_1^2 + 8x_2 + 5} - 1\\
&\qquad Y = 0.9063x_1 + 0.4226x_2\\
&\qquad Z = 0.4226x_1 - 0.9063x_2\\
&\qquad 0 \le e_{x_1} \le 10, \quad 0 \le e_{x_2} \le 10
\end{aligned}
\tag{22}
$$

According to the improved two-stage framework of EBDO, in the first stage, firstly, evidence variables are converted into random variables using the equal areas method. Taking the design point ($e_{x_1} = 5$, $e_{x_2} = 5$) as an example, Fig. 7 illustrates the BPA structures and their corresponding PDFs after transformation. For the sake of convenience in calculating the probability and cumulative densities of a random variable, the RBF metamodel is constructed and used to replace the piecewise linear PDF of the random variable. Then, the reliability analysis is conducted by HMV and the RBDO problem with random variables is solved by SORA. In the second stage, the improved algorithm in Section 3.2 is used for calculating the *Pl* of constraint violation. In this work, the vertex method is employed to calculate the values of $g_{\min}(D^t)$ and $g_{\max}(D^t)$ when they cannot be assigned the recorded values directly. Finally, the EBDO optimum in (22) is obtained by using the DIRECT.

Comparatively, the EBDO problem in this example is directly solved by using DIRECT without searching for the RBDO optimum, which is termed as one-stage EBDO in this study. In addition, the two-stage EBDO method with the hypothetical normal distribution (ND; Mourelatos and Zhou 2006), called as two-stage EBDO with ND in this study, is also adopted to solve the problem in this example. For both of the two-stage methods, the number of maximum iterations is set to 5 for the optimization in the second stage. To make a fair comparison, the number of maximum iterations for the one-stage method is also set to 5. Besides, the improved algorithm for calculating the *Pl* of failure is employed in the one-stage method. Comparative results obtained by the three methods under different values of p_f are provided in Table 2. To demonstrate the accuracy of these methods, genetic algorithm

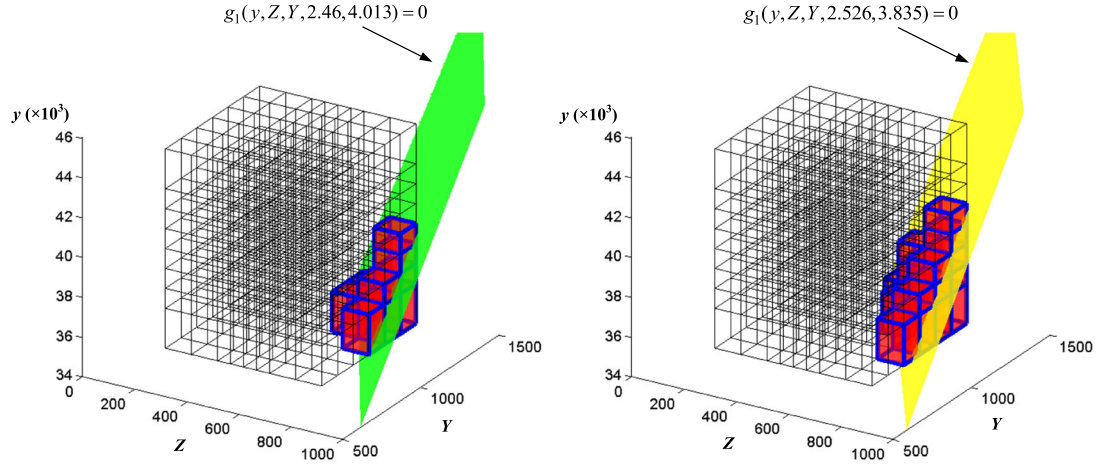

(a) The RBDO optimum in the first stage

(b) The EBDO optimum in the second stage

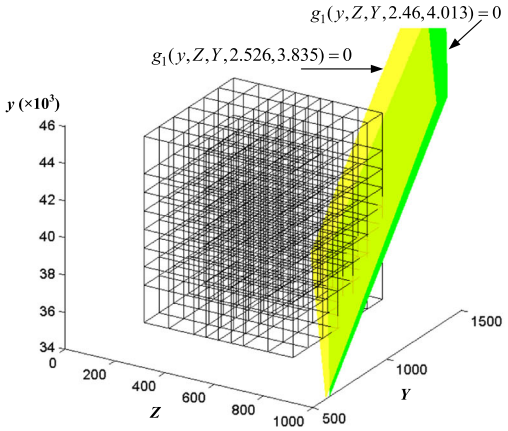

(c) Comparison of the RBDO and EBDO optimums

Fig. 10 Limit-state surfaces of $g_1 = 0$ at the RBDO and EBDO optimums under $p_f = 0.01$ in example 2

(GA) is applied to search for the relatively accurate EBDO optimum. In GA, the population size is set to 100, and it stops if the average relative change of the best fitness function value is less than 10^{-6}. For the cases with $p_f = 0.01$, 0.1, and 0.2, the final EBDO optimums obtained by GA are −1.6426, −1.8199, and −1.95267 under 116, 87, and 85 generations, respectively.

As shown in Table 2, compared with the two-stage method with ND, the RBDO optimum obtained by the improved two-stage method is closer to its EBDO optimum under each case. Therefore, the improvement in the first stage of the two-stage EBDO method is beneficial. To take an example, Fig. 8a, b show the RBDO and EBDO optimums obtained by the improved two-stage method under $p_f = 0.01$, respectively. The failure focal elements in *FD*s are represented by green rectangle blocks in Fig. 8a, b. The relative location of the RBDO and EBDO optimums is illustrated in Fig. 8c. It can be observed that they are very close, which will be helpful for obtaining the EBDO optimum in the second stage.

To check the efficiency of the improved two-stage method, the total call number of the objective and constraint functions in each stage during the whole EBDO solving process is summarized in Table 2. As shown in Table 2, compared with the two-stage methods, the total number of function calls in the one-stage method is the least under cases with the number of maximum iterations 5. However, the EBDO optimums obtained by the one-stage method under these cases are the most conservative. We try to increase the number of maximum iterations in the one-stage method. When it arrives at 50, the less conservative optimum can be obtained. However, much more function calls are required. Compared with the two-stage method with ND, the improved method needs fewer function calls except the case of $p_f = 0.01$. On the other side, the EBDO

Table 6 Comparison of efficiency for calculating *Pl* of failure in example 2

p_f	The vertex method			The gradient-based method		
	Algorithms of calculating *Pl* of failure	Number of each constraint function calls		Algorithms of calculating *Pl* of failure	Number of optimizer calls for each constraint	
		g_1	g_2		g_1	g_2
0.01	Algorithm involving all focal elements	3072	2304	Algorithm without records	135	2
	The improved algorithm	**168**	**12**	The improved algorithm	**81**	**2**
0.1	Algorithm involving all focal elements	3072	2304	Algorithm without records	398	197
	The improved algorithm	**444**	**256**	The improved algorithm	**220**	**108**
0.2	Algorithm involving all focal elements	3072	2304	Algorithm without records	517	239
	The improved algorithm	**564**	**344**	The improved algorithm	**280**	**124**

optimums obtained by these two methods are close. Therefore, the improved two-stage framework of EBDO is computationally more efficient to some extent.

On the other hand, the efficiency of the improved algorithm for calculating the *Pl* of failure is checked. As mentioned in Section 3.2, $g_{\min}(D^t)$ and $g_{\max}(D^t)$ can be calculated by the vertex method or the gradient-based method. In this example, for the vertex method, the *Pl* of failure at the EBDO optimum is calculated by the improved algorithm and the traditional algorithm involving all focal elements, respectively. Table 3 lists the number of each constraint function calls during the calculation. Compared with the traditional algorithm, the improved algorithm needs much fewer calls for each constraint function under each case of p_f. For the gradient-based method, we compare the improved algorithm and the original algorithm without records (Mourelatos and Zhou 2006). From Table 3, it can be found that the improved algorithm needs less number of optimizer calls than the algorithm without records for constraints g_1 and g_2. For constraint g_3, the same number of optimizer calls is needed in the two algorithms. This is because no type 1 focal elements in Fig. 1 exist in the *FD*. Thus, it is demonstrated that the improved algorithm has a high efficiency on calculating the *Pl* of failure.

4.2 A cantilever beam example

A cantilever beam in vertical and lateral bending (Mourelatos and Zhou 2006) is presented and used to test the improved two-stage framework of EBDO. Figure 9 shows the cantilever beam. The vertical and lateral loads Y and Z are applied to the tip of the cantilever beam. The length L of the beam is 100 in. The width w and thickness t of the cross section of the beam are deterministic design variables. Assuming the material density and the beam length are constant, the objective is to minimize the weight of the beam, which can be transformed into the minimization of $f = w \times t$. Two non-linear failure modes are considered: yielding at the fixed end of the beam and the tip displacement. The allowable value of the tip displacement is $D_0 = 2.5$ in. The EBDO problem is shown as:

$$\begin{aligned} &\text{find}: w, t \\ &\min: f = w \times t \\ &s.t. \quad Pl\{g_i(\boldsymbol{d}, \boldsymbol{P}) < 0\} \le p_f, i = 1, 2 \\ &\quad g_1(y, Z, Y, w, t) = y - \left(\frac{600}{wt^2} \times Y + \frac{600}{w^2 t} \times Z\right) \\ &\quad g_2(E, Z, Y, w, t) = D_0 - \frac{4L^3}{Ewt}\sqrt{\left(\frac{Y}{t^2}\right)^2 + \left(\frac{Z}{w^2}\right)^2} \\ &\quad 0 \le w, t \le 5 \end{aligned} \tag{23}$$

where g_1 and g_2 are the limit state functions. The deterministic design variables $\boldsymbol{d} = [w, t]$. In this example, in order to test the advantage of the improved method without the assumption that unknown evidence variables and parameters obey the normal distribution, the BPA structures of evidence parameters $\boldsymbol{P} = [Z, y, Y, E]$ are modified to distinguish them from those with normal distribution. E denotes the Young modulus, and y is the yield strength. The BPA structures are listed in Table 4.

Similar to example 1, the EBDO problem of the cantilever beam is solved by three EBDO methods. For both of the two-stage methods, the number of maximum iterations is set

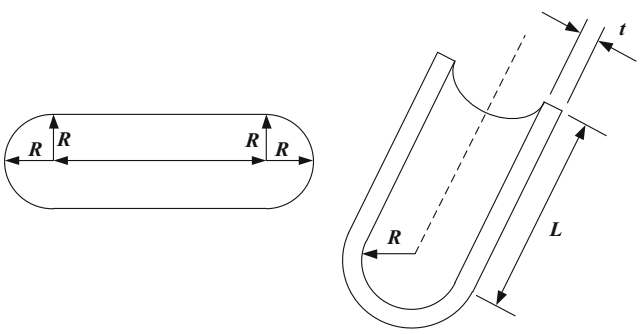

Fig. 11 Thin-walled pressure vessel

Table 7 BPA structures for R, L and t

R		L		t	
Interval	BPA (%)	Interval	BPA (%)	Interval	BPA (%)
$[e_R–6.0, e_R4.5]$	1	$[e_L–12, e_L–9]$	2	$[e_t–0.4, e_t–0.3]$	5
$[e_R–4.5, e_R–3.0]$	19	$[e_L–9, e_L–6]$	20	$[e_t–0.3, e_t–0.2]$	15
$[e_R–3.0, e_R]$	30	$[e_L–6, e_L]$	28	$[e_t–0.2, e_t]$	30
$[e_R, e_R + 3.0]$	30	$[e_L, e_L + 6]$	28	$[e_t, e_t–0.2]$	30
$[e_R + 3.0, e_R + 4.5]$	19	$[e_L + 6, e_L + 9]$	20	$[e_t–0.2, e_t–0.3]$	15
$[e_R + 4.5, e_R + 6.0]$	1	$[e_L + 9, e_L + 12]$	2	$[e_t–0.3, e_t–0.4]$	5

to 10 for the optimization in the second stage. The number of maximum iterations for the one-stage method is also set to 10. The improved algorithm for calculating the Pl of failure is employed in the one-stage method. Comparative results under different values of p_f are presented in Table 5. In order to validate the accuracy of these methods, GA is employed to search for the relatively accurate EBDO optimums. For the cases with $p_f = 0.01$, 0.1, and 0.2, the final EBDO optimums gained by GA are 9.6852, 8.8444, and 8.5267 under 169, 130, and 121 generations, respectively.

As shown in Table 5, compared with the two-stage method with ND, the RBDO optimum obtained by the improved two-stage method is closer to its EBDO optimum under almost each case. This proves that the improvement in the first stage of the two-stage EBDO method is beneficial. To take an example, Fig. 10a, b illustrate the limit-state surfaces of g_1 at the RBDO and EBDO optimums obtained by the improved two-stage method under $p_f = 0.01$. Because no evidence variables exist in this example, the RBDO and EBDO optimums of the deterministic design variables w and t can be adopted to define different limit-state surfaces with respect to evidence parameters. In Fig. 10a, the green plane denotes the limit-state surface $g_1(y, Z, Y, 2.46, 4.013) = 0$ at the RBDO optimum. In Fig. 10b, the yellow plane denotes the limit-state surface $g_1(y, Z, Y, 2.526, 3.835) = 0$ at the EBDO optimum. The red cubes in Fig. 10a, b represent the failure focal elements. The relative location of the two limit-state surfaces at the RBDO and EBDO optimums is displayed in Fig. 10c. It can be observed that the two planes are very close.

From Table 5, with the number of maximum iterations 10, the total number of function calls in the one-stage method is the least under $p_f = 0.1$ and 0.2. When its number of maximum iterations is increased to 30, less conservative optimums are obtained. However, much more function calls are required. Compared with the two-stage method with ND, the improved method needs fewer function calls under all cases. On the other hand, the EBDO optimums obtained by these two methods are close. Therefore, it is verified that the improved two-stage framework of EBDO is more efficient.

After calculating the Pl of failure at the EBDO optimum by different algorithms, Table 6 lists the number of each constraint function calls during the calculation in the vertex method and the number of optimizer calls for each constraint function in the gradient-based method. As seen in Table 6, compared to the traditional algorithm, the improved algorithm needs much fewer calls of each constraint function under all cases for the vertex method. For the gradient-based method, the number of optimizer calls for each constraint in the improved algorithm is not more than those in the algorithm without records under all cases. Accordingly, it is verified that the improved algorithm has a high efficiency on calculating the Pl of failure.

4.3 A pressure vessel example

A thin-walled pressure vessel (Mourelatos and Zhou 2006) is provided and employed to test the proposed two-stage framework of EBDO. As shown in Fig. 11, the pressure vessel has hemispherical ends and the design variables are the radius R, the length L, and the thickness t. The objective is to maximize the volume of the vessel. The vessel is to withstand a specified internal pressure P. The yielding of the material in both the

Table 8 BPA structures for P and Y

P		Y ($\times 10^5$)	
Interval	BPA (%)	Interval	BPA (%)
[800, 850]	1	[2.08, 2.21]	5
[850, 900]	20	[2.21, 2.34]	20
[900, 1000]	30	[2.34, 2.6]	30
[1000, 1100]	30	[2.6, 2.86]	25
[1100, 1150]	18	[2.86, 2.99]	10
[1150, 1200]	1	[2.99, 3.12]	10

Table 9 Comparative results under different cases in example 3

p_f	EBDO methods	Max. iterations	RBDO optimum			EBDO optimum			EBDO objective	*Pl* of failure					Total number of function calls in each stage
			R	L	t	R	L	t	f	Pl_1	Pl_2	Pl_3	Pl_4	Pl_5	
0.15	One-stage	5	/	/	/	6.778	29	0.430	5.489E + 03	0.0306	0.0461	0.0528	0.048	0.1195	40,017
		15	/	/	/	7.034	29.678	0.430	6.070E + 03	0.0335	0.0482	0.1094	0.1050	0.1195	1,843,159
	Two-stage with ND	5	10.042	34.714	0.400	/	/	/	/	/	/	/	/	0.638	326 + 175,881
	Improved two-stage	5	7.026	29.297	0.446	7.048	30.408	0.446	**6.212E + 03**	0.0107	0.0394	0.1434	0.1050	0.1195	650 + 258,715
0.3	One-stage	5	/	/	/	7.296	29	0.489	6.477E + 03	0	0.0142	0.0754	0.1905	0.1195	38,821
		15	/	/	/	7.546	34.682	0.410	8.004E + 03	0.0500	0.0619	0.2814	0.2000	0.1030	920,537
	Two-stage with ND	5	11.408	35.841	0.400	/	/	/	/	/	/	/	/	/	350 + 151,409
	Improved two-stage	5	8.027	30.513	0.400	8.383	32.291	0.417	**9.596E + 03**	0.0495	0.0637	0.2588	0.2600	0.0145	477 + 142,795

Table 10 Comparison of efficiency for calculating *Pl* of failure in example 3

p_f	The vertex method						The gradient-based method					
	Algorithms of calculating *Pl* of failure	Number of each constraint function calls					Algorithms of calculating *Pl* of failure	Number of optimizer calls for each constraint				
		g_1	g_2	g_3	g_4	g_5		g_1	g_2	g_3	g_4	g_5
0.15	Algorithm involving all focal elements	20,736	20,736	1728	144	144	Algorithm without records	299	654	172	43	43
	The improved algorithm	**680**	**1456**	**376**	**112**	**112**	The improved algorithm	**136**	**346**	**91**	**25**	**25**
0.3	Algorithm involving all focal elements	20,736	20,736	1728	144	144	Algorithm without records	800	1094	247	53	27
	The improved algorithm	**1736**	**2408**	**560**	**128**	**80**	The improved algorithm	**411**	**570**	**138**	**29**	**17**

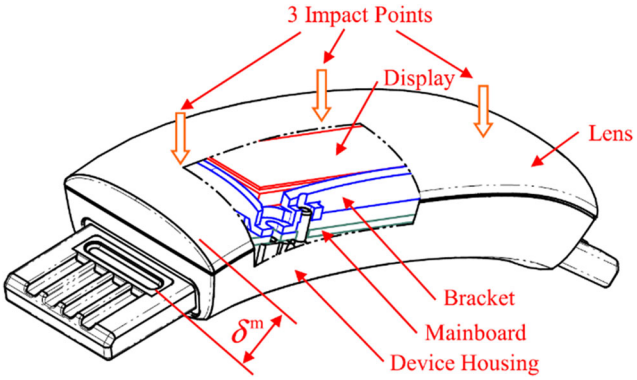

Fig. 12 A wearable smart watch

circumferential and radial directions should be avoided. Some geometric constraints are also taken into consideration. The material yield strength is Y. The safety factor SF is set to 2. The EBDO problem in this example is shown as:

$$
\begin{aligned}
&find: e_R, e_L, e_t\\
&\max: \quad f = \frac{4}{3}\pi e_R^3 + \pi e_R^2 e_L\\
&s.t. \quad Pl\{g_i(R,L,t,P,Y) < 0\} \le p_f, \quad i = 1,\ldots,5\\
&\quad g_1 = 1.0 - \frac{P(R+0.5t)SF}{2tY}\\
&\quad g_2 = 1.0 - \frac{P(2R^2+2Rt+t^2)SF}{(2Rt+t^2)Y}\\
&\quad g_3 = 1.0 - \frac{L+2R+2t}{60}\\
&\quad g_4 = 1.0 - \frac{R+t}{12}\\
&\quad g_5 = 1.0 - \frac{5t}{R}\\
&\quad 0.4 \le e_t \le 2.0\\
&\quad 6.0 \le e_R \le 24\\
&\quad 12 \le e_L \le 48
\end{aligned}
\tag{24}
$$

Different from the former two examples, this example has both epistemic uncertainty variables (i.e., R, L and t) and epistemic uncertainty parameters (i.e., P and Y). To test the improved method without assuming that unknown evidence variables and parameters obey the normal distribution, the BPA structures of evidence variables and parameters are modified to distinguish them from those with normal distribution. The BPA structures are provided in Tables 7 and 8.

Similar to example 1, the EBDO problem of the pressure vessel is solved by three EBDO methods. For both of the two-stage methods, the number of maximum iterations is set to 5 for the optimization in the second stage. The number of maximum iterations for the one-stage method is also set to 5. The improved algorithm for calculating the Pl of failure is employed in the one-stage method. Comparative results under different values of p_f are presented in Table 9. Moreover, GA is used to search for the relatively accurate EBDO optimums to check the accuracy of these three methods. The final EBDO optimums from GA are 6238.04 and 9665.26 for the cases with $p_f = 0.15$ and 0.3 under 174 and 138 generations, respectively.

As shown in Table 9, with the number of maximum iterations 5, the two-stage method with ND cannot obtain an EBDO optimum. However, the RBDO optimum obtained by the improved two-stage method is very close to its EBDO optimum under each case. Thus, the improvement in the first stage of the two-stage EBDO method is important and helpful. Moreover, under $p_f = 0.3$, the improved two-stage method requires fewer function calls than the two-stage method with ND. Therefore, the improved method is more efficient for quickly obtaining an EBDO optimum. Considering the maximization problem in (24), the EBDO optimums of the improved two-stage method are less conservative than those of the one-stage method.

During calculating the Pl of failure at the EBDO optimum, Table 10 gives the number of each constraint function calls in the vertex method and the number of optimizer calls for each constraint function in the gradient-based method. As seen in Table 10, for the vertex method, the number of

Table 11 BPA structures for P_1, P_2, P_3, P_4 and P_5

P_1 ($\times 10^2$ Mpa)	P_2 ($\times 10^2$ Mpa)	P_3 ($\times 10$ Mpa)	P_4 (W)	P_5 (W)	BPA (%)
[104, 106]	[218, 222]	[218, 228]	[0.09, 0.11]	[0.09, 0.11]	10
[106, 108]	[222, 226]	[228, 238]	[0.11, 0.13]	[0.11, 0.13]	10
[108, 110]	[226, 230]	[238, 248]	[0.13, 0.15]	[0.13, 0.15]	30
[110, 112]	[230, 234]	[248, 258]	[0.15, 0.17]	[0.15, 0.17]	30
[112, 114]	[234, 238]	[258, 268]	[0.17, 0.19]	[0.17, 0.19]	10
[114, 116]	[238, 242]	[268, 298]	[0.19, 0.21]	[0.19, 0.21]	10

each constraint function calls in the improved algorithm is much less than that in the traditional algorithm under all cases. For the gradient-based method, compared with the algorithm without records, the improved algorithm needs fewer optimizer calls under all cases. Hence, it is demonstrated that the improved algorithm can efficiently calculate the *Pl* of failure.

4.4 Engineering example: Electronic packaging design for a smart watch

In this section, the improved two-stage framework is applied to an electronic packaging design for a smart watch as shown in Fig. 12 (Huang et al. 2016). The optimization objective is to obtain an optimal thickness of the watch to satisfy the wearing comfort. Some extreme conditions with hard impact and high temperature should be considered to keep watch working reliably. For this purpose, three points on the screen are considered as experiment points to hit against with three identical steel balls. The material stress in each point, Γ_i^N for $i = 1, 2, 3$, should be less than the corresponding yield strength $\Gamma^{\mathrm{Display}}$. In order to ensure the normal operation of the watch, the maximum temperatures of two chips T_1 and T_2 are required to be less than allowable value T^{Chip} when the operating temperature of device is set to 50 °C. Moreover, the maximum stress Γ^H of the solder should not be higher than the allowable value Γ^{Solder}. The thicknesses of the device, main board, bracket, display, and lens are chosen as design variables, which are denoted by X_i for $i = 1, 2,\ldots,5$. The Young Modulus of the main board, display and lens are selected as evidence parameters, which are denoted by P_i for $i = 1, 2, 3$. The power dissipations of two chips are also treated as evidence parameters, which are denoted by P_4 and P_5. The BPA structures of evidence parameters are provided in Table 11. There are six constraints and each of their target failure probabilities is 0.1. The EBDO problem is formulated as follows:

$$
\begin{aligned}
&find: X_i,\ \ i = 1,\ \ 2,\ \ \ldots,\ \ 5\\
&\min:\quad f = X_1 + X_2 + X_3 + X_4 + X_5\\
&s.t.\quad\ Pl\{g_i(\boldsymbol{X},\boldsymbol{P}) < 0\} \le p_f,\qquad i = 1,\ldots,6\\
&\qquad g_1 = \Gamma^{\mathrm{Display}} - \Gamma_1^{\mathrm{N}}(\boldsymbol{X},\boldsymbol{P})\\
&\qquad g_2 = \Gamma^{\mathrm{Display}} - \Gamma_2^{\mathrm{N}}(\boldsymbol{X},\boldsymbol{P})\\
&\qquad g_3 = \Gamma^{\mathrm{Display}} - \Gamma_3^{\mathrm{N}}(\boldsymbol{X},\boldsymbol{P})\\
&\qquad g_4 = \Gamma^{\mathrm{Solser}} - \Gamma^{\mathrm{H}}(\boldsymbol{X},\boldsymbol{P})\\
&\qquad g_5 = T^{\mathrm{Chip}} - T_1(\boldsymbol{X},\boldsymbol{P})\\
&\qquad g_6 = T^{\mathrm{Chip}} - T_2(\boldsymbol{X},\boldsymbol{P})\\
&\Gamma^{\mathrm{Display}} = 82.0\mathrm{Mpa},\quad \Gamma^{\mathrm{Solser}} = 62.8\mathrm{Mpa},\quad T^{\mathrm{Chip}} = 95^{\circ}\mathrm{C}\\
&1.0\mathrm{mm} \le X_1 \le 2.0\mathrm{mm},\ \ 0.8\mathrm{mm} \le X_2 \le 1.6\mathrm{mm},\ \ 0.6\mathrm{mm} \le X_3 \le 2.2\mathrm{mm}\\
&1.2\mathrm{mm} \le X_4 \le 2.4\mathrm{mm},\ \ 1.2\mathrm{mm} \le X_5 \le 2.4\mathrm{mm}
\end{aligned}
\tag{25}
$$

In order to improve the optimization efficiency, a quadratic response surface function is established for each constraint utilizing 65 FEM samples. The expressions of constructed response surface functions can be found in Huang et al. (2016). Similar to mathematical examples, the EBDO problem of the smart watch is solved by three EBDO methods. For both of the two-stage methods, the number of maximum iterations is set to 10 for the optimization in the second stage. The number of maximum iterations for the one-stage method is also set to 10. The improved algorithm for calculating the *Pl* of failure is employed in the one-stage method. Comparative results under $p_f = 0.1$ are presented in Table 12. In addition, the EBDO optimum obtained by GA is 6.8046 under 164 generations.

As shown in Table 12, with the number of maximum iterations 10, the two-stage method with ND and one-stage method cannot obtain an EBDO optimum. However, the RBDO optimum obtained by the improved two-stage method is close to its EBDO optimum. So it is demonstrated that the improvement in the first stage of the two-stage method is helpful and beneficial. Furthermore, compared with the two-stage method with ND, fewer function calls are required by the improved two-stage method. Hence, the improved method is more efficient for quickly finding an EBDO optimum.

During calculating the *Pl* of failure at the EBDO optimum, Table 13 gives the number of each constraint function calls in the vertex method and the number of optimizer calls for each constraint function in the gradient-based method. As seen in Table 13, for the vertex method, the number of each constraint function calls in the improved algorithm is much less than that in the traditional algorithm. For the gradient-based method, compared with the algorithm without records, the improved algorithm needs the same calls of the optimizer, because focal elements with types 1 and 3 do not exist in the *FD*s for all constraints.

4.5 Analysis and discussion

As illustration of the improved algorithm for calculating the *Pl* of failure in Fig. 4, it can be found that the focal elements with type 3, which intersect with the limit-state curves or surfaces, will have a large influence on the computational efficiency. As the number of focal elements with type 3 increases, the number of limit-state function calls and the computational cost will raise. Generally, the EBDO optimum is close to the limit-state curves or surfaces. For the one-stage EBDO method, the initial search region is often far from the limit-state curves or surfaces. During its initial optimization iterations, a few focal elements with type 3 exist and the number of limit-state function calls is small. With the increasing of iterations, the number of limit-state function calls will increase rapidly. On the other hand, for the two-stage EBDO method, the RBDO optimum obtained in the first stage is in the vicinity of the EBDO optimum and considered as the initial design point in the second stage. To obtain an

Table 12 Comparative results under $p_f = 0.1$ in example 4

EBDO methods		One-stage		Two-stage with ND	Improved two-stage
Max. iterations		10	30	10	10
RBDO optimum	X_1	/	/	1.000	1.609
	X_2	/	/	0.800	0.872
	X_3	/	/	1.896	2.200
	X_4	/	/	1.200	1.200
	X_5	/	/	1.255	1.200
EBDO optimum	X_1	/	1.778	/	1.431
	X_2	/	0.889	/	0.810
	X_3	/	2.111	/	2.191
	X_4	/	1.201	/	1.201
	X_5	/	1.201	/	1.201
Pl of failure	Pl_1	/	0	/	0
	Pl_2	/	0	/	0
	Pl_3	/	0	/	0
	Pl_4	/	0	/	0
	Pl_5	/	0	/	0
	Pl_6	/	0	/	0
EBDO objective		/	7.181	/	**6.833**
Total number of function calls in each stage		4581	33,536	3931 + 11,775	3442 + 4726

EBDO optimum, usually only few iterations (such as 5–10 iterations) are required in the second stage. Because its initial design point is close to the limit-state curves or surfaces, the second stage will need more function calls than the one-stage method when the same few iterations are set (such as the number of maximum iterations 5 and 10). This can be verified by the statistical data in Tables 2, 5, 9 and 12.

Additionally, to obtain a relatively accurate EBDO optimum, the number of maximum iterations needs to be increased for the one-stage method. From the statistical data in Tables 2, 5, 9 and 12, it can be found that much more function calls are required for the one-stage method, although the relatively accurate EBDO optimums can be obtained.

For the two-stage method with ND, it is assumed that each dimension of the *FD* is equal to some times the standard derivation of a hypothetical normal distribution. Therefore, the RBDO optimums obtained by the two-stage method with ND may be farther from the limit-state curves or surfaces than those obtained by the improved method. As shown in Tables 2, 5, 9 and 12, compared with the two-stage method with ND, the RBDO optimum obtained by the improved method is closer to its EBDO optimum under each case. This proves that the improvement in the first stage is beneficial. On the other hand, as shown in Tables 3, 6, 10 and 13, it is demonstrated that the improved algorithm has a higher efficiency on calculating the *Pl* of constraint failure than the existing algorithm in Mourelatos and Zhou (2006). Also, the improved method requires fewer function calls in the second stage than the two-stage method with ND under all cases. This proves that the improvement in the second stage is also beneficial.

Table 13 Comparison of efficiency for calculating *Pl* of failure in example 4

The vertex method							The gradient-based method						
Algorithms of calculating *Pl* of failure	Number of each constraint function calls						Algorithms of calculating *Pl* of failure	Number of optimizer calls for each constraint					
	g_1	g_2	g_3	g_4	g_5	g_6		g_1	g_2	g_3	g_4	g_5	g_6
Algorithm involving all focal elements	144	144	144	12	144	144	Algorithm without records	2	2	2	2	2	2
The proposed algorithm	**6**	**6**	**6**	**3**	**6**	**6**	The proposed algorithm	**2**	**2**	**2**	**2**	**2**	**2**

Meanwhile, as shown in Tables 2, 5, 9 and 12, with the same iterations in the second stage, the improved two-stage method can search for the EBDO optimums in all examples; while the two-stage method with ND fails in the pressure vessel and smart watch examples. Moreover, in the mathematical and beam examples, it can be seen that compared with the two-stage method with ND, the improved method needs fewer total function calls except the only one case of the mathematical example with $p_f = 0.01$. In these two examples, the improved method obtains less conservative EBDO optimums than the two-stage method with ND. Nevertheless, the EBDO optimums obtained by the improved method are the closest to those obtained by GA, which are used as the reference values to check the accuracy of all the methods. Overall, the improved two-stage method is more efficient and the accuracy of its solutions can be ensured.

5 Conclusions and further work

This paper makes two improvements on the original two-stage framework of EBDO in Mourelatos and Zhou (2006): (1) the first stage is improved to get rid of the assumption that unknown evidence variables and parameters obey the normal distribution. Specifically, the equal areas method is employed to convert evidence variables into random variables. Then, a RBDO problem with random variables is defined and solved by SORA; (2) in the second stage, the original algorithm for the calculation of the *Pl* of constraint violation is improved by continuously recording the minimum and maximum values of limit-state functions to achieve higher computational efficiency. Numerical and engineering examples are given to test the advantages of the improved two-stage framework of EBDO. Results show that the RBDO optimum obtained in the first stage by the improved framework is very close to its EBDO optimum in the second stage. The improvement in the first stage is proved to be beneficial to quickly obtain the EBDO optimum. Meanwhile, the higher efficiency of the improved algorithm for calculating the *Pl* of constraint failure is demonstrated. Overall, the improved two-stage framework is more efficient for obtaining an accurate EBDO optimum.

For multimodal function optimization problems, the RBDO solution of the first stage may not be in the vicinity of the actual EBDO optimum. As a global optimizer, DIRECT has a potential to find the actual EBDO optimum if the initial search region is not in its vicinity. However, large computational cost may be needed. On the other hand, the SORA method and the DIRECT optimizer used in the improved two-stage method cannot solve multi-objective problems. Thus, the improved two-stage framework of EBDO is not suitable for multimodal or multi-objective optimization problems under epistemic uncertainty.

Additionally, although the computational efficiency of the two-stage framework is improved significantly, the number of objective and constraint functions calls is still large. As discussed in Section 4.5, the number of focal elements which intersect with the limit-state curves or surfaces has a large influence on the number of limit-state function calls. Generally, the total number of function calls will increase as the increasing of the number of evidence variables and parameters. For high-dimensional problems involving many evidence variables and parameters (such as 10^2–10^3), huge computational cost will be taken. In practical engineering applications, metamodeling techniques need to be used to replace computer-based simulations in the improved two-stage framework.

As part of further work, some other approaches for design under uncertainty can be taken into account in the two-stage framework, such as partially converged simulations, fusion with experimental data, and epistemic uncertainty in computer models.

Acknowledgements This research was supported by the National Natural Science Foundation of China [grant numbers 51675196 and 51721092].

References

Agarwal H, Renaud JE, Preston EL, Padmanabhan D (2004) Uncertainty quantification using evidence theory in multidisciplinary design optimization. Reliab Eng Syst Saf 85(1):281–294

Alyanak E, Grandhi R, Bae HR (2008) Gradient projection for reliability-based design optimization using evidence theory. Eng Optim 40(10):923–935

Bae HR, Grandhi RV, Canfield RA (2004a) An approximation approach for uncertainty quantification using evidence theory. Reliab Eng Syst Saf 86(3):215–225

Bae HR, Grandhi RV, Canfield RA (2004b) Epistemic uncertainty quantification techniques including evidence theory for large-scale structures. Comput Struct 82(13):1101–1112

Bai YC, Han X, Jiang C, Liu J (2012) Comparative study of metamodeling techniques for reliability analysis using evidence theory. Adv Eng Softw 53(11):61–71

Du XP (2006) Uncertainty analysis with probability and evidence theories. In: Proceedings of the 2006 ASME International Design Engineering Technical Conference & Computers and Information in Engineering Conference, ASME Paper DETC2006–99078

Du XP (2008) Unified uncertainty analysis by the first order reliability method. ASME J Mech Des 130(9):091401

Du XP, Chen W (2004) Sequential optimization and reliability assessment method for efficient probabilistic design. ASME J Mech Des 2:225–233

Hao P, Wang YT, Liu C, Wang B, Wu H (2017) A novel non-probabilistic reliability-based design optimization algorithm using enhanced chaos control method. Comput Methods Appl Mech Eng 318:572–593

Hardy RL (1971) Multiquadric equations of topography and other irregular surfaces. J Geophys Res 76(8):1905–1915

Huang HZ, Zhang X (2009) Design optimization with discrete and continuous variables of aleatory and epistemic uncertainties. ASME J Mech Des 131(3):031006

Huang HZ, He LP, Liu Y, Xiao NC, Li YF, Wang ZL (2013) Possibility and evidence-based reliability analysis and design optimization. Am. J Eng Appl Sci 6(1):95–136

Huang ZL, Jiang C, Zhou YS, Luo Z, Zhang Z (2016) An incremental shifting vector approach for reliability-based design optimization. Struct Multidiscip Optim 53(3):523–525

Huang ZL, Jiang C, Zhang Z, Fang T, Han X (2017) A decoupling approach for evidence-theory-based reliability design optimization. Struct Multidiscip Optim 56(3):647–661. https://doi.org/10.1007/s00158-017-1680-x

Jiang C, Bi RG, Lu GY, Han X (2013a) Structural reliability analysis using non-probabilistic convex model. Comput Methods Appl Mech Eng 254(2):83–98

Jiang C, Zhang Z, Han X, Liu J (2013b) A novel evidence-theory-based reliability analysis method for structures with epistemic uncertainty. Comput Struct 129:1–12

Jones DR, Perttunen CD, Stuckman BE (1993) Lipschitzian optimization without the Lipschitz constant. J Optim Theory Appl 73(11):157–181

Kiureghian AD, Ditlevsen O (2009) Aleatory or epistemic? Does it matter? Struct Saf 31(2):105–112

Li F, Luo Z, Rong JH, Zhang N (2013) Interval multi-objective optimization of structures using adaptive kriging approximations. Comput Struct 119(4):68–84

Li G, Lu Z, Xu J (2015) A fuzzy reliability approach for structures based on the probability perspective. Struct Saf 54:10–18

Meng D, Li YF, Huang HZ, Wang Z, Liu Y (2015a) Reliability-based multidisciplinary design optimization using subset simulation analysis and its application in the hydraulic transmission mechanism design. ASME J Mech Des 137(5):051402

Meng Z, Li G, Wang BP, Hao P (2015b) A hybrid chaos control approach of the performance measure functions for reliability-based design optimization. Comput Struct 146:32–43

Moore RE (1966) Interval analysis. Prentice-Hall, Englewood Cliffs

Mourelatos ZP, Zhou J (2006) A design optimization method using evidence theory. ASME J Mech Des 128(4):901–908

Oberkampf WL, Helton JC (2002) Investigation of evidence theory for engineering applications. In: AIAA non-deterministic approaches forum. No. AIAA 2002–1569, Denver, April

Oberkampf WL, Helton JC, Sentz K (2001) Mathematical representations of uncertainty. In: AIAA non-deterministic approaches forum, no. AIAA 2001–1645, Seattle, WA, April

Rosenblatt M (1952) Remarks on a multivariate transformation. Ann Math Stat 23(3):470–472

Salehghaffari S, Rais-Rohani M, Marin EB, Bammann DJ (2013) Optimization of structures under material parameter uncertainty using evidence theory. Eng Optim 45(9):1027–1041

Sentz K, Ferson S (2002) Combination of evidence in Dempster-Shafer theory. Sandia National Laboratories, Albuquerque

Shafer G (1976) A mathematical theory of evidence. Princeton university press, Princeton

Shan S, Wang GG (2008) Reliable design space and complete single-loop reliability-based design optimization. Reliab Eng Syst Saf 93(8):1218–1230

Srivastava RK, Deb K, Tulshyan R (2013) An evolutionary algorithm based approach to design optimization using evidence theory. ASME J Mech Des 135(8):081003

Wang Z, Wang P (2014) A maximum confidence enhancement based sequential sampling scheme for simulation-based design. ASME J Mech Des 136(2):021006

Wu J, Luo Z, Zhang Y, Zhang N, Chen L (2013) Interval uncertain method for multibody mechanical systems using chebyshev inclusion functions. Int J Numer Meth Eng 95(7):608–630

Xiao M, Gao L, Xiong HH, Luo Z (2015) An efficient method for reliability analysis under epistemic uncertainty based on evidence theory and support vector regression. J Eng Des 26(10–12):1–25

Yager R, Fedrizzi M, Kacprzyk J (1994) Advances in the Dempster-Shafer theory of evidence. Wiley, New York

Yang X, Liu Y, Zhang Y, Yue Z (2015) Probability and convex set hybrid reliability analysis based on active learning Kriging model. Appl Math Model 39(14):3954–3971

Yang X, Liu Y, Gao Y (2016) Unified reliability analysis by active learning kriging model combining with random-set based Monte Carlo simulation method. Int J Numer Meth Eng 108(11):1343–1361

Yang X, Liu Y, Ma P (2017) Structural reliability analysis under evidence theory using the active learning kriging model. Eng Optim:1–17. https://doi.org/10.1080/0305215X.2016.1277063

Yao W, Chen X, Huang Y, Gurdal Z, van Tooren M (2013) Sequential optimization and mixed uncertainty analysis method for reliability-based optimization. AIAA J 51(9):2266–2277

Yi P, Zhu Z (2016) Step length adjustment iterative algorithm for inverse reliability analysis. Struct Multidiscip Optim 54(4):1–11

Youn BD, Choi KK, Park YH (2003) Hybrid analysis method for reliability-based design optimization. ASME J Mech Des 125(2):221–232

Youn BD, Choi KK, Du L (2005) Enriched performance measure approach for reliability-based design optimization. AIAA J 43(4):874–884

Youn BD, Xi Z, Wang P (2008) Eigenvector dimension reduction (EDR) method for sensitivity-free probability analysis. Struct Multidiscip Optim 37(1):13–28

Zadeh LA (1965) Fuzzy sets. Inf Control 8(3):338–353

Zhang X, Huang HZ (2010) Sequential optimization and reliability assessment for multidisciplinary design optimization under aleatory and epistemic uncertainties. Struct Multidiscip Optim 40(1):165–175

Zhang Z, Jiang C, Han X, Hu D, Yu S (2014) A response surface approach for structural reliability analysis using evidence theory. Adv Eng Softw 69:37–45

Zhang Z, Jiang C, Wang GG, Han X (2015) First and second order approximate reliability analysis methods using evidence theory. Reliab Eng Syst Saf 137:40–49